7-18-2011

Enhancement of optical emission from laser-induced plasmas by combined spatial and magnetic confinement

L. B. Guo
University of Nebraska-Lincoln and Huazhong University of Science and Technology

W. Hu
University of Nebraska-Lincoln

B. Y. Zhang
University of Nebraska-Lincoln

X. N. He
University of Nebraska-Lincoln

C. M. Li
University of Nebraska-Lincoln and Huazhong University of Science and Technology

See next page for additional authors

Authors
L. B. Guo, W. Hu, B. Y. Zhang, X. N. He, C. M. Li, Y. S. Zhou, Z. X. Cai, X. Y. Zeng, and Yongfeng Lu

Enhancement of optical emission from laser-induced plasmas by combined spatial and magnetic confinement

L.B. Guo,[1,2] W. Hu,[1] B.Y. Zhang,[1] X.N. He,[1] C.M. Li,[1,2] Y.S. Zhou,[1] Z.X. Cai,[2] X.Y. Zeng[2] and Y.F. Lu[1,*]

[1]*Department of Electrical Engineering, University of Nebraska-Lincoln, Lincoln, NE 68588-0511 USA*
[2]*School of Optoelectronics Science and Engineering, Huazhong University of Science and Technology, Wuhan, Hubei 430074, China*
**ylu2@unl.edu*

Abstract: To enhance optical emission in laser-induced breakdown spectroscopy, both a pair of permanent magnets and an aluminum hemispherical cavity (diameter: 11.1 mm) were used simultaneously to magnetically and spatially confine plasmas produced by a KrF excimer laser in air from pure metal and alloyed samples. High enhancement factors of about 22 and 24 in the emission intensity of Co and Cr lines were acquired at a laser fluence of 6.2 J/cm^2 using the combined confinement, while enhancement factors of only about 11 and 12 were obtained just with a cavity. The mechanism of enhanced optical emission by combined confinement, including shock wave in the presence of a magnetic field, is discussed. The Si plasmas, however, were not influenced by the presence of magnets as Si is hard to ablate and ionize and hence has less free electrons and positive ions. Images of the laser-induced Cr and Si plasmas show the difference between pure metallic and semiconductor materials in the presence of both a cavity and magnets.

OCIS codes: (300.6365) Spectroscopy, laser-induced breakdown; (350.5400) Plasmas.

References and links

1. G. Asimellis, S. Hamilton, A. Giannoudakos, and M. Kompitsas, "Controlled inert gas environment for enhanced chlorine and fluorine detection in the visible and near-infrared by laser-induced breakdown spectroscopy," Spectrochimica Acta Part B. **60**(7-8), 1132–1139 (2005).
2. L. J. Radziemski and D. A. Cremers, *Laser Induced Plasma and Applications* (Marcel Dekker, New York, 1989).
3. H. Zhang, F. Y. Yueh, and J. P. Singh, "Laser-induced breakdown spectrometry as a multimetal continuous-emission monitor," Appl. Opt. **38**(9), 1459–1466 (1999).
4. J. P. Singh and S. N. Thakur, *Laser-Induced breakdown Spectroscopy* (Elsevier Science, Oxford, 2007).
5. Yu. P. Razier, *Laser-Induced Discharge Phenomena* (Consultants Bureau New York, 1977).
6. A. K. Knight, N. L. Scherbarth, D. A. Cremers, and M. J. Ferris, "Characterization of Laser-Induced Breakdown Spectroscopy (LIBS) for Application to Space Exploration," Appl. Spectrosc. **54**(3), 331–340 (2000).
7. G. Arca, A. Ciucci, V. Palleschi, S. Rastelli, and E. Tognoni, "Trace element analysis in water by the laser-induced breakdown spectroscopy techinique," Appl. Spectrosc. **51**(8), 1102–1105 (1997).
8. T. X. Phuoc and F. P. White, "Laser induced spark for measurements of the fuel-to-air ratio of a combustible mixture," Fuel **81**(13), 1761–1765 (2002).
9. D. A. Cremers, L. J. Radziemski, and T. R. Loree, "Spectrochemical analysis of liquids using the laser spark," Appl. Spectrosc. **38**(5), 721–729 (1984).
10. D. Anglos, V. Zafiropulos, K. Melessanaki, M. J. Gresalfi, and J. C. Miller, "Laser-induced breakdown spectroscopy for the analyses of 150-year old daguerreotypes," Appl. Spectrosc. **56**(4), 423–432 (2002).
11. A.W. Miziolect, V. Palleschi and I. Schechter eds., *Laser-Induced Breakdown Spectroscopy (LIBS) - Fundamentals and Applications* (Cambridge University Press, Cambridge, 2006).
12. D. A. Cremers and L. J. Radzeimki, *Handbook of Laser Induced Breakdown Spectroscopy* (Wiley, 2006).
13. D. N. Stratis, K. L. Eland, and S. M. Angel, "Enhancement of aluminum, titanium, and iron in glass using pre-ablation spark dual-pulse LIBS," Appl. Spectrosc. **54**(12), 1719–1726 (2000).
14. J. Scaffidi, W. Pearman, J. C. Carter, and S. M. Angel, "Observations in collinear femtosecond-nanosecond dual-pulse laser-induced breakdown spectroscopy," Appl. Spectrosc. **60**(1), 65–71 (2006).

#148392 - $15.00 USD Received 3 Jun 2011; revised 25 Jun 2011; accepted 27 Jun 2011; published 7 Jul 2011

15. J. Scaffidi, J. Pender, W. Pearman, S. R. Goode, B. W. Colston, Jr., J. C. Carter, and S. M. Angel, "Dual-pulse laser-induced breakdown spectroscopy with combinations of femtosecond and nanosecond laser pulses," Appl. Opt. **42**(30), 6099–6106 (2003).
16. R. E. Russo, X. L. Mao, J. J. Gonzalez, and S. S. Mao, "Femtosecond laser ablation ICR-MS," J. Anal. At. Spectrom. **17**(9), 1072–1075 (2002).
17. X. K. Shen, H. Wang, Z. Q. Xie, Y. Gao, H. Ling, and Y. F. Lu, "Detection of trace phosphorus in steel using laser-induced breakdown spectroscopy combined with laser-induced fluorescence," Appl. Opt. **48**(13), 2551–2558 (2009).
18. X. N. He, W. Hu, C. M. Li, L. B. Guo, and Y. F. Lu, "Generation of high-temperature and low-density plasmas for improved spectral resolutions in laser-induced breakdown spectroscopy," Opt. Express **19**(11), 10997–11006 (2011).
19. H. Sobral, M. Villagrán-Muniz, R. Navarro-González, and A. C. Raga, "Temporal evolution of the shock wave and hot core air in laser induced plasma," Appl. Phys. Lett. **77**(20), 3158–3160 (2000).
20. X. K. Shen, J. Sun, H. Ling, and Y. F. Lu, "Spectroscopic study of laser-induced Al plasmas with cylindrical confinement," J. Appl. Phys. **102**(9), 093301 (2007).
21. A. M. Popov, F. Colao, and R. Fantoni, "Enhancement of LIBS signal by spatially confining the laser-induced plasma," J. Anal. At. Spectrom. **24**(5), 602 (2009).
22. A. M. Popov, F. Colao, and R. Fantoni, "Spatial confinement of laser-induced plasma to enhance LIBS sensitivity for trace elements determination in soils," J. Anal. At. Spectrom. **25**(6), 837–848 (2010).
23. L. B. Guo, C. M. Li, W. Hu, Y. S. Zhou, B. Y. Zhang, Z. X. Cai, X. Y. Zeng, and Y. F. Lu, "Plasma confinement by hemispherical cavity in laser-induced breakdown spectroscopy," Appl. Phys. Lett. **98**(13), 131501 (2011).
24. V. N. Rai, A. K. Rai, F. Y. Yueh, and J. P. Singh, "Optical emission from laser-induced breakdown plasma of solid and liquid samples in the presence of a magnetic field," Appl. Opt. **42**(12), 2085–2093 (2003).
25. L. I. Sedov, *Similarity and Dimensional Methods in Mechanics* (Cleaver Hume, London, 1959).
26. V. N. Rai, M. Shukla, and H. C. Pant, "An x-ray biplanar photodiode and the x-ray emission from magnetically confined laser produced plasma," Pramana J. Phys. **52**(1), 49–65 (1999).
27. F. F. Chen, *Introduction to Plasma Physics* (Plenum, New York, 1974).
28. V. N. Rai, A. K. Rai, F. Y. Yueh, and J. P. Singh, "Optical emission from laser-induced breakdown plasma of solid and liquid samples in the presence of a magnetic field," Appl. Opt. **42**(12), 2085–2093 (2003).
29. X. K. Shen, Y. F. Lu, T. Gebre, H. Ling, and Y. X. Han, "Optical emission in magnetically confined laser-induced breakdown spectroscopy," J. Appl. Phys. **100**(5), 053303 (2006).
30. G. Han and P. T. Murray, "Laser-plasma interactions in 532 nm ablation of Si," J. Appl. Phys. **88**(2), 1184–1186 (2000).

1. Introduction

Within the past decades, laser-induced breakdown spectroscopy (LIBS) has become a well-established and powerful optical emission spectroscopy (OES) analytical technique [1–5]. As a useful analytical tool, LIBS is used extensively in various areas such as remote detection, hostile environment monitoring, and cultural heritage conservation [6–10]. Researchers are paying more attention to LIBS as a diagnostic method for elemental analysis as it is characterized by fast, real-time, in *situ*, low invasiveness, and multi-elemental diagnosis, normally without the need for sample preparation [11,12]. However, one of its major drawbacks is its low sensitivity, which seriously hinders further improving the limit of detection (LOD) and restricts the further development and application of LIBS. To enhance the LIBS sensitivity, ultrashort-pulse and dual-pulse LIBS have been developed in recent years [13–18].

The signal and sensitivity of LIBS can be significantly increased by using ultrashort-pulse and dual-pulse schemes. However, there are two drawbacks: one is the increased complexity of the LIBS setup, and the other is the increased cost of using more than one laser. Besides adopting the newest laser or adding lasers, another handy, flexible, and cost effective method is combining the spatial and magnetic confinement of plasmas, which can effectively improve the sensitivity of LIBS in a facile way. As is well known, a shock wave is produced with a plasma when a sample is ablated by a laser pulse [19]. On one hand, the plasma is confined by the magnetic field; on the other hand, the shock wave spreads out at a very high speed, and will be reflected back when encountering walls and will compress the plasma [20]. Combining these two effects, the plasma is compressed into the center, resulting in highly increased collision rates among particles within the plasma which leads to an increase in the number of atoms in high-energy states and, hence, enhanced emission spectra intensity [21, 22]. In the past, researchers only studied the plasma confinement effects using either spatial or magnetic confinement. For instance, our previous research [23] studied the enhancement of

#148392 - $15.00 USD Received 3 Jun 2011; revised 25 Jun 2011; accepted 27 Jun 2011; published 7 Jul 2011

plasmas confined with an aluminum hemispherical cavity, resulting in an enhancement factor of 12 for Mn lines of low-concentration Mn element. Rai *et al.* [24] have studied the magnetic field confinement effect in air with a homemade magnetic device, achieving a maximum enhancement factor of 2 for metal alloy samples. The aim of this work was to investigate the enhancement effects by applying combined spatial and magnetic confinements in LIBS. Laser-induced plasmas were produced in a hemispherical cavity located in an externally applied static magnetic field between a pair of permanent magnets. The OES and fast imaging of the plasma plumes were investigated to study the evolution of the plasmas.

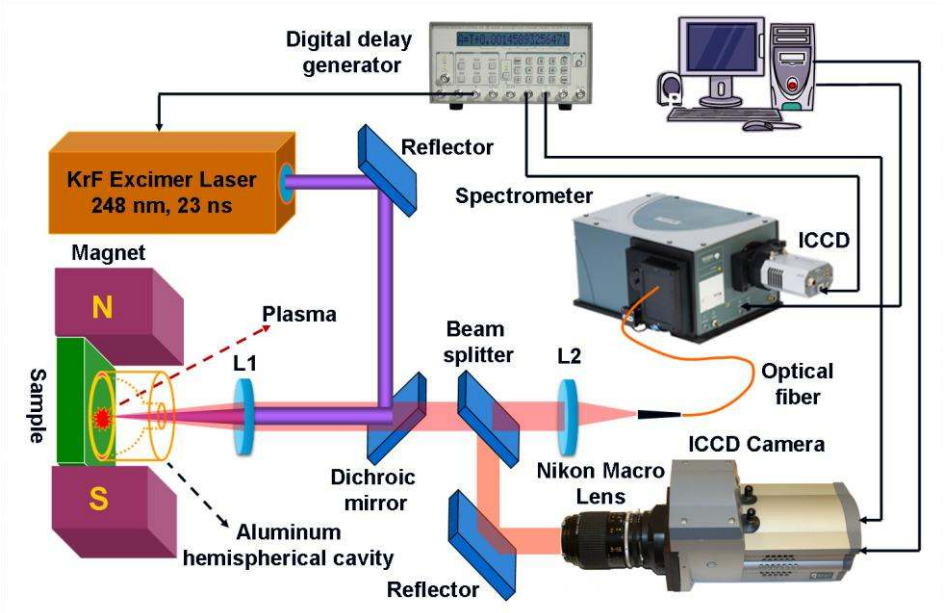

Fig. 1. Schematic diagram of the experiment setup.

2. Experimental methods

2.1 Experiment setup

Figure 1 shows a schematic diagram of the experimental setup. The experiments were conducted in open air. A KrF Excimer laser (Lambda Physik, Compex 205, wavelength: 248 nm, pulse duration: 23 ns) was used for plasma generation. The laser beam was reflected by a dichroic mirror, and focused normally to a target surface through a 2 mm hole at the top of an aluminum hemispherical cavity (diameter: 11.1 mm) by a UV-grade quartz lens (L1) with a 15 cm focal length. The dichroic mirror was reflective to the laser beam but transparent to the other wavelengths. The cavity was placed tightly on the target surface which was sandwiched between two permanent magnets of 3 × 1 × 1 $inch^3$. The magnets were fixed in a plastic structure with a space of 20 cm between them, in which a nearly uniform magnetic field of 0.8 T was produced. A plasma plume was generated and expanded from the center of the cavity which was located in the magnetic field. The plume size was about several millimeters. We only studied the optical emissions at the center of the plasma where the plasma is the brightest and most stable. The emission spectra were collected through the top hole and then split up by a beam splitter. One of the split beams which passed through the beam splitter was coupled to an optical fiber by a UV-grade quartz lens (L2) with a focal length of 6 cm. The optical fiber, with a core diameter of 100 μm, was coupled to a spectrometer (Andor Tech., Shamrock 303i). A grating of the spectrometer of 2400 lines/mm was used which has a spectral resolution of 0.05 nm. A 512 × 512 pixel intensified charge-coupled device (ICCD) (Andor Tech., iStar, DH-712) was attached to the exit focal plane of the spectrograph. Another light

#148392 - $15.00 USD Received 3 Jun 2011; revised 25 Jun 2011; accepted 27 Jun 2011; published 7 Jul 2011

beam, which was reflected by the beam splitter, was reflected to an ICCD camera (Andor Tech., iStar, DH-734) and imaged by a Nikon Macro lens (105 mm, *f*/2.8D). Both of the ICCDs were operated in the gated mode. The laser, the spectrometer, and the ICCD cameras were controlled by a digital delay generator and operated in the external trigger mode for synchronization with a repetition rate of 5 Hz. Data and image acquisitions were performed using a computer. The purities of the Co, Cr, and Si targets were 99.993%, 99.95%, and 99.999%, respectively. An alloy of a Cupro-Nickel target (NIST 1276a) with Cu, Ni, and Mg contents of 66.7%, 30.0%, and 120 ppm, respectively, was used in this study.

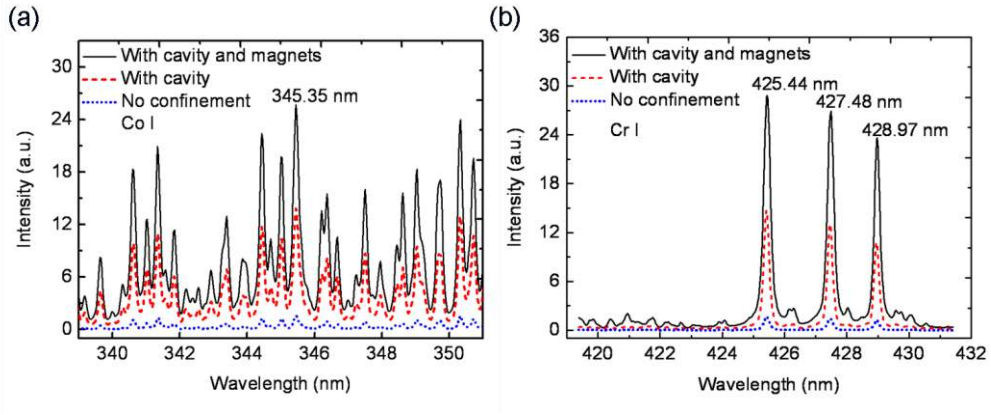

Fig. 2. Time-integrated spectra from (a) Co and (b) Cr targets with the presence of both a hemispherical cavity and magnets (solid curve), with the cavity only (short dashed curve), and without confinement (short dotted curve) at a laser fluence of 6.2 J/cm^2.

3. Results and discussion

3.1 Time-integrated OES of Co and Cr plasmas from pure metals

First, the time-integrated OES spectra of laser-induced Co and Cr plasmas from pure metals were measured to demonstrate the intensity enhancement effects. The emission spectra of pure Co and Cr metal samples were obtained in two spectral ranges of 339–351 nm and 419–431 nm with both a hemispherical cavity and magnets (solid curves), with the hemispherical cavity only (short dashed curves), and with no confinement (short dotted curves) under otherwise the same conditions, as shown in Figs. 2(a) and 2(b), respectively. The spot size of the focused laser beam was about 2.0 × 1.0 mm^2 with a laser fluence of 6.2 J/cm^2. Both the gate delay and gate width of the ICCD camera were 8 μs. The signals were accumulated with consecutive ablations by 30 pulses to reduce the standard deviation. The emission intensities for the Co (345.35 nm) and Cr (425.44, 427.48 and 428.97 nm) atomic lines were all obviously enhanced with the presence of either type of confinement. The intensities of Co emission lines in the spectrum obtained by pure cobalt using both the hemispherical cavity and magnets (solid curves in Fig. 2(a)) exceeded a factor of 16 larger than the case without confinement (short dotted curves in Fig. 2(a)), while a factor of 9 was obtained when using the hemispherical cavity only. Similar to the Co sample, an increase in intensities of Cr I lines of about 17 and 10 were obtained with both the cavity and magnets and the cavity only, respectively. The transition configuration for the Co atomic lines were $3p^6 3d^8(^3\mathrm{F})4s$ - $3p^6 3d^8(^3\mathrm{F})4p$, and that for three Cr atomic lines was $3d^5(^6\mathrm{S})4s$ - $3d^5(^6\mathrm{S})4p$, where the $3p^6 3d^8(^3\mathrm{F})4s$ and $3d^5(^6\mathrm{S})4s$ are the ground states of the Co and Cr atoms.

#148392 - $15.00 USD Received 3 Jun 2011; revised 25 Jun 2011; accepted 27 Jun 2011; published 7 Jul 2011

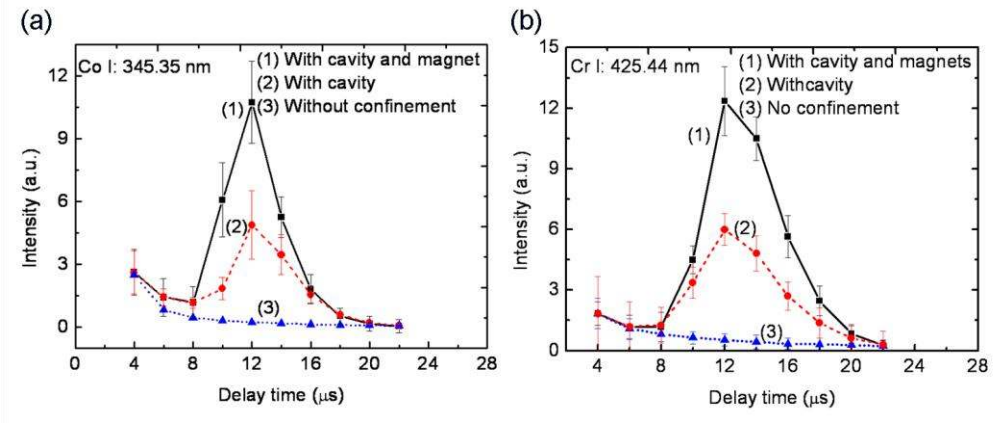

Fig. 3. Emission intensity of (a) Co atomic lines (345.35 nm) and (b) Cr atomic lines (425.44 nm) as a function of time delay, using both a hemispherical cavity and magnets (square dots and solid curve), using the cavity only (circle dots and short dashed curve), and without confinement (triangle dots and short dotted) at a laser fluence of 6.2 J/cm^2.

3.2 Temporal evolution of emission intensities for Co and Cr atomic lines from pure metal samples

The laser-induced breakdown plasmas are a pulsed source. The temporally resolved emission spectra were investigated to further understand the temporal evolution of the plasmas. OES spectra at different time delays were obtained by adjusting the time delay and gate width of the ICCD detector. Figures 3(a) and 3(b) show the temporal evolution of the emission intensities of the Co (345.35 nm) and Cr (425.44 nm) atomic lines using both the cavity and magnets (square dots and solid curve), using a cavity only (circle dots and short dashed curve), and without confinement (triangle dots and short dotted). The data recording started at a delay time of 4 μs and ended at 22 μs, with a gate width of 2 μs and a step of 2 μs for delay times. As shown in Fig. 3(a), for delay times from 10 to 16 μs, the Co atomic line was significantly enhanced when both the cavity and magnets were present. A maximum enhancement factor of about 22 was achieved at a time delay of 12 μs, while an enhancement factor of only about 11 was obtained with the cavity only. Similarly for the Co sample, at the same time delay of 12 μs, a maximum enhancement factor of about 24 was achieved for the Cr I lines with both the cavity and magnets present, while an enhancement factor of about 12 was obtained with the cavity only.

Obviously, significant enhancements of the emission signals from the pure metallic plasmas produced in the hemispherical cavity combined with a pair of permanent magnets have been obtained, leading to a higher detection sensitivity. The main reason for this effect is related to the combined effect of spatial and magnetic confinements. In the experiment, a shock wave is produced by the initial explosive pressure along with the plasma generation and spreads out as a spherical wave with a high supersonic velocity [25]. When the spherical wave encounters the hemispherical cavity wall, it is uniformly reflected and travels back towards the plasma center. At the same time, because an external magnetic field is applied to the metallic laser-induced plasmas, according to the magnetohydrodynamic (MHD) theory, the electrons and ions within the plasmas are influenced by the Lorentz force. From MHD equations indicate that a magnetic field exerts a magnetic pressure, $B^2/2\,\mu_0$, perpendicular to field lines, where B is the ambient magnetic field and μ_0 is permeability of vacuum. Thus, plasmas tend to be tied to magnetic field lines, rendering the decelerated expansion and diffusion of plasmas. The deceleration of the plasma expansion under the influence of a magnetic field can be given as

$$\frac{v_2}{v_1} = (1-\frac{1}{\beta})^{1/2}, \qquad (1)$$

#148392 - $15.00 USD Received 3 Jun 2011; revised 25 Jun 2011; accepted 27 Jun 2011; published 7 Jul 2011

where v_1 and v_2 are, respectively, the asymptotic plasma expansion velocity in the absence and in the presence of the magnetic field [26]. The parameter β of the plasma is given by

$$\beta = \frac{8\pi nkT_e}{B^2}, \tag{2}$$

where n is the electron density (cm^{-3}), k is the Boltzmann constant, T_e is the electron temperature (eV), and B is the magnetic field (G). The plasma parameter β is the ratio of particle pressure and magnetic field pressure, which indicates the size of the diamagnetic effect [27,28]. When $\beta = 1$, the plasma would be stopped by the magnetic field. In the case of high β, the magnetic confinement would not be obvious. In the case of low β plasma, the magnetic confinement would be effective [29]. In our experiments, the plasma was simultaneously confined by both mechanisms. The plasma plume was compressed even further than the case using spatial confinement alone. The plasma density at center region was drastically increased, which led to an increased number of the collisions among particles within the plasma. This enhanced collision in turn resulted in an increased number of excited atoms, and consequently increased the temperature at the center of the plasma. Therefore, the emission intensities of the pure metallic plasmas with combined spatial and magnetic confinements were further enhanced, resulting in a higher detection sensitivity.

3.3 Time-integrated OES and temporal evolution of emission intensity for Si atomic line

In addition to pure metallic samples, the OES of laser-induced semiconductive Si (288.16 nm) was measured with both the cavity and magnets (solid curve), with a cavity only (short dashed curve), and with no confinement (short dotted curve) under otherwise the same condition as that for the pure metallic samples, as shown in Fig. 4(a). The emission intensities for the Si atomic line (288.16 nm) were obviously enhanced with the presence of either type of confinement. However, it was different from the pure metallic samples in that the intensity enhancements were almost the same whether using a hemispherical cavity and magnets together or using a hemispherical cavity only.

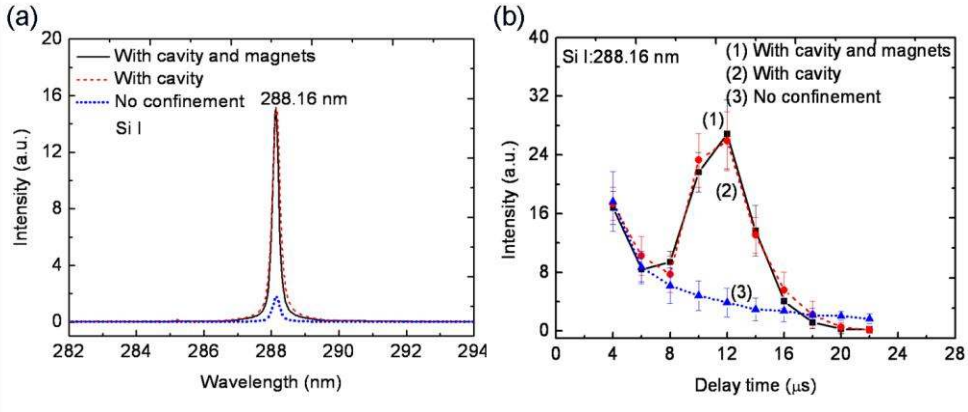

Fig. 4. (a) Time-integrated spectra from Si targets with the presence of both a hemispherical cavity and magnets (solid curve), with the cavity only (short dashed curve), and without confinement (short dotted curve) at a laser fluence of 6.2J/cm^2. (b) Emission intensity of Si I atomic lines (288.16 nm) as a function of time delay, using both a hemispherical cavity and magnets (square dots and solid curve), using the cavity only (circle dots and short dashed curve), and without confinement (triangle dots and short dotted) at a laser fluence of 6.2 J/cm^2.

Figure 4(b) shows the time evolution of the emission intensity of the Si atomic line (288.16 nm) using both the cavity and magnets (square dots and solid curve), using a cavity only (circle dots and short dashed curve), and without confinement (triangle circle dots and short dotted). In the case with both the cavity and magnets, the best enhancement time appears at the same time delay of 12 μs. However, the maximum enhancement factor only reached 10,

#148392 - $15.00 USD Received 3 Jun 2011; revised 25 Jun 2011; accepted 27 Jun 2011; published 7 Jul 2011

which is much smaller than the metallic materials. The reason can be found in the Si plasmas, which are not as influenced by the magnetic field, because Si is more difficult to be ablated and ionized due to its high ionization potential, resulting in less amount of free electrons and positive ions within the Si plasmas [30]. The temporal evolution of the Si atomic line (288.16 nm) was nearly independent of the magnetic field.

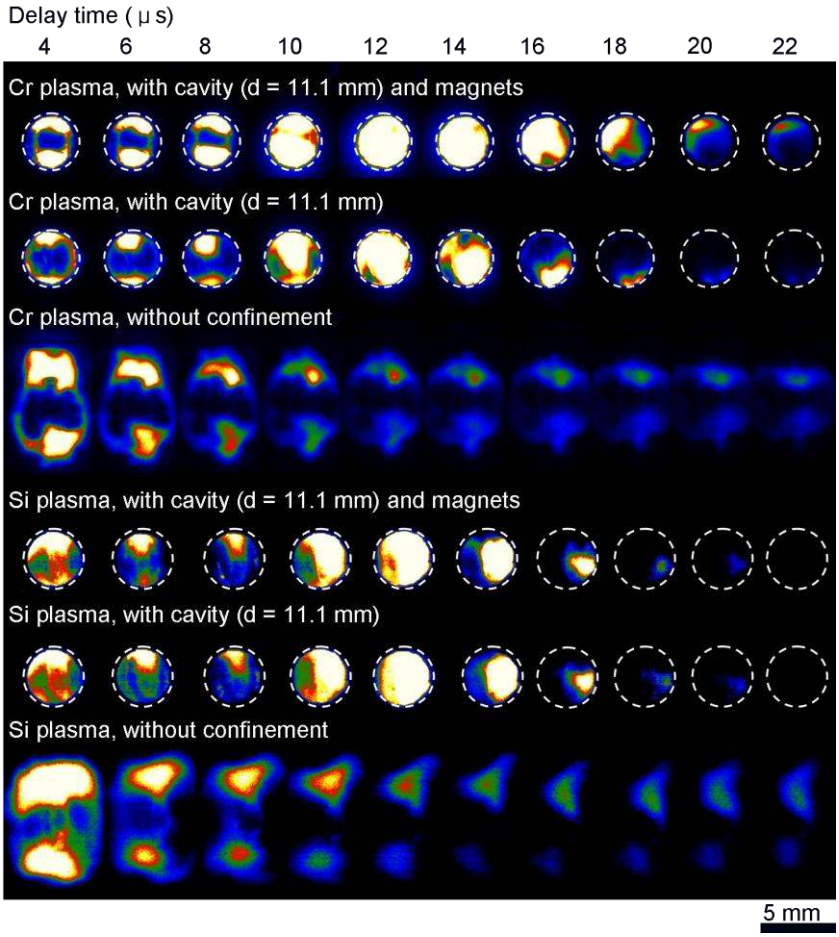

Fig. 5. Fast images of laser-induced Cr and Si plasmas using both a hemispherical cavity and magnets (first and fourth row), using the cavity only (second and fifth row), and without confinement (third and sixth row), respectively, at a laser fluence of 6.2 J/cm^2.

3.4 Fast imaging of laser-induced Cr and Si plasmas with different confinements

The time evolution of the plasma plumes from pure metallic and semiconductor samples were directly observed using fast imaging. Figure 5 shows the images of Cr plasmas on a relative intensity scale with the presence of both the cavity and magnets (first row), with a cavity only (second row), and without confinement (third row). The image recording started at delay time of 4 μs and ended at 22 μs, with a gate width of 2 μs and a step of 2 μs for delay times. When a cavity was used, the images were taken through the hole on top of the cavity, indicated by the dotted circles. As can be seen from the images, the size of the luminous plasma without confinement was approximately 5 mm in diameter. By comparing the plasma images with (first and second rows) and without (third row) confinement, the plasma was obviously compressed towards the center. It also shows that the plasma plumes with both the cavity and magnets or with the cavity only became obviously brighter during 10–16 μs, and the brightest time appeared at a delay time of 12 μs, consistent with the result of the time-resolved OES

#148392 - $15.00 USD Received 3 Jun 2011; revised 25 Jun 2011; accepted 27 Jun 2011; published 7 Jul 2011

curves of Cr. The plasma plume with both confinements was much brighter, stable, and lasted longer than with case with the cavity only, apparently due to the magnetic confinement. In contrast, the plasma plume without confinement decayed gradually. This demonstrates that the enhancement factor, when using both the cavity and magnets, is much stronger than the cases just using the cavity alone or with no confinement. However, the Si plasma images with both the cavity and magnets (fourth rows) and those with a cavity only (fifth row) show no detectable difference in the plasma evolutions. This demonstrates that the plasma emission intensity enhancement of Si is dominated only by the hemispherical cavity rather than the magnets, consistent to the result of time-resolved OES curve of Si.

3.5 Temporal evolution of emission intensities for Cu and Ni atomic lines from an alloy sample

Apart from pure sample detection, the alloy of a Cupro-Nickel target (NIST 1276a, Cu, Ni, and Mg contents of 66.7%, 30.0%, and 120 ppm) was also investigated with the same parameters of the laser fluence and ICCD setting up. The results of Cu and Ni are also similar to the pure metallic samples, as Fig. 6 (a) shows. At a time delay of 12 μs, a maximum enhancement factor of about 22 was achieved for the Cu I lines with both the cavity and magnets present. Similarly, an enhancement factor of just about 11 was obtained with the cavity only. It was almost the same for Ni I lines detection.

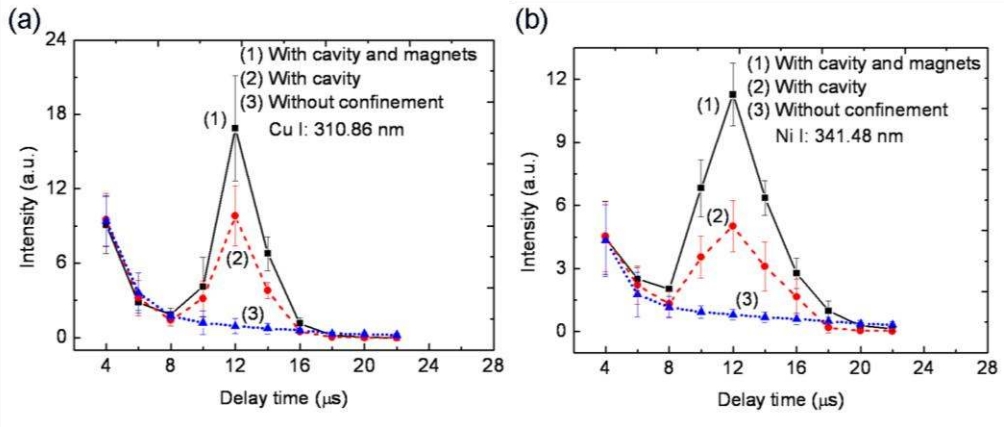

Fig. 6. Emission intensity of (a) Cu atomic (310.86 nm) lines and (b) Ni atomic lines (341.48 nm) from an alloy sample as a function of time delay, using both a hemispherical cavity and magnets (square dots and solid curve), using the cavity only (circle dots and short dashed curve), and without confinement (triangle dots and short dotted) at a laser fluence of 6.2 J/cm^2.

3.6 Temporal evolution of emission intensity for trace-level Mg atomic line from the alloy sample

The enhanced effect of trace elements has been scrutinized. Figure 7 shows the temporal evolution of Mg (concentration: 120 ppm) in the Cupro-Nickel target (NIST 1276a) with the same ICCD detector settings except that the laser fluence was increased to 6.9 J/cm^2. Between 8 and 12 μs, the intensity of the Mg (518.36 nm) atomic line was significantly enhanced. A maximum enhancement factor of 15 was achieved with both the cavity and magnets, while an enhancement factor of about 7 was achieved with the cavity only. The additional enhancement by adding the magnets is the same as that for the pure metals. Thus, the combination of plasma confinements using both the hemispherical cavity and magnets cannot only significantly enhance the intensity of the major compositions but also enhance the trace-level elements.

#148392 - $15.00 USD Received 3 Jun 2011; revised 25 Jun 2011; accepted 27 Jun 2011; published 7 Jul 2011

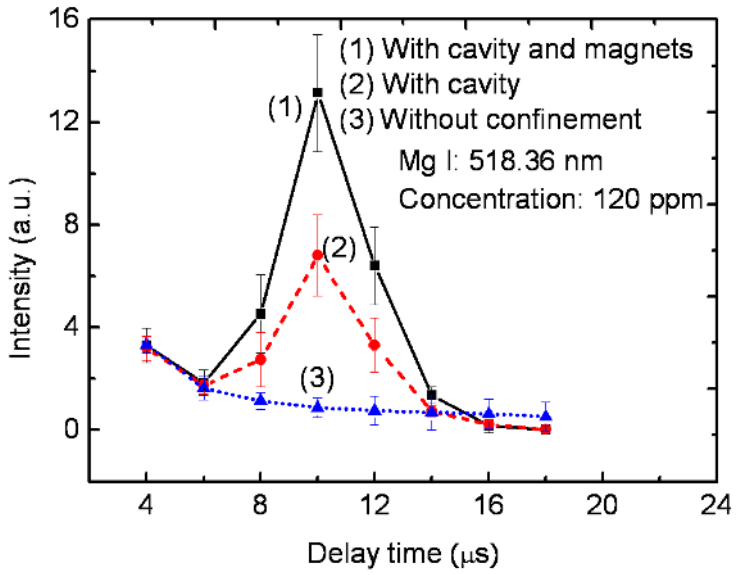

Fig. 7. Emission intensity of trace-level Mg I atomic lines (288.16 nm) from an alloy sample as a function of time delay, using both a hemispherical cavity and magnets combined (square dots and solid curve), using the cavity only (circle dots and short dashed curve), and without confinement (triangle dots and short dotted) at a laser fluence of 6.9 J/cm^2.

4. Conclusions

In summary, the combined spatial and magnetic confinements using both the hemispherical cavity and permanent magnets in LIBS were studied. Significant enhancements in LIBS of pure metallic samples such as Co and Cr were observed. The maximum enhancement factor for the atomic lines exceeded 22 at a delay time of 12 μs with both the cavity and magnets, while more than 11 was obtained with the cavity only at a laser fluence of 6.2 J/cm^2. This obviously shows that the enhancement effect using both the hemispherical cavity and magnets is much stronger than the cases using the cavity only. Similar results were obtained for an alloy sample. However, it shows that the magnetic field has no influence on Si samples. The images of the pure metallic plasma plumes directly show that the plumes confined by both the cavity and the magnetic field are more effectively compressed to the hemispherical cavity center and become brighter, demonstrating the special effects of combining spatial and magnetic confinements. In contrast, under otherwise the same condition, the Si plasma images exhibit no appreciable change between those with both a cavity and magnets and those with a cavity only. This illustrates that the enhancement of plasma emission from Si is only determined by the hemispherical cavity rather than the magnets, due to the low ionization of Si. The results of this research have shown promise for further improving the LIBS sensitivity.

Acknowledgement

This research work was financially supported by Office of Naval Research (MURI N00014-05-1-0432 and N00014-09-1-0943).

#148392 - $15.00 USD Received 3 Jun 2011; revised 25 Jun 2011; accepted 27 Jun 2011; published 7 Jul 2011